Available online at www.sciencedirect.com
SCIENCE DIRECT®
Journal of Magnetic Resonance 169 (2004) 73–84
JMR Journal of Magnetic Resonance
www.elsevier.com/locate/jmr

A new adaptive subband decomposition approach for automatic analysis of NMR data

El-Hadi Djermoune,[a,*] Marc Tomczak,[a] and Pierre Mutzenhardt[b]

[a] *Centre de Recherche en Automatique de Nancy, CRAN-UMR CNRS 7039, Université Henri Poincaré, Nancy 1, B.P. 239, 54506, Vandoeuvre-lès-Nancy Cedex, France*

[b] *Laboratoire de Méthodologie RMN, Université Henri Poincaré, Nancy 1, B.P. 239, 54506 Vandoeuvre-lès-Nancy Cedex, France*

Received 23 October 2003; revised 15 March 2004
Available online 10 May 2004

Abstract

This paper presents a non-iterative, fast, and almost automated time-data analysis method for NMR spectroscopy, based on a new adaptive implementation of high resolution methods used in spectral subbands. It is intended to avoid the choice of the decimation factor (or the width of the spectral windows) which, in the case of a uniform decomposition, strongly conditions the estimation results, and to diminish the computational burden. It is achieved through successive decimation/estimation stages each followed by a test procedure in order to decide whether or not the process should continue. The proposed test is based on a local spectral flatness measure of the estimation residuals. This stop-criterion involves an a posteriori validation of the estimation, thus the method proposed allows one to obtain a better detection rate at a lower complexity comparatively to other stopping rules, while preserving a reasonable estimation variance. Moreover, the reliability of the fitting algorithms considered is improved, by decreasing the influence of the model order and the number of false detections. Finally, the method is more efficient than Fourier transform (FT) at low signal-to-noise ratio (SNR). The effectiveness of the method is demonstrated by analyzing a simulation signal and raw carbon-13 experimental data.

Keywords: Time-data analysis; Linear prediction; High-order Yule–Walker estimation; ^{13}C NMR; Adaptive subband decomposition; Spectral flatness

1. Introduction

In spite of the considerable progress of the nuclear magnetic resonance (NMR) in the last 20 years, the Fourier transform (FT) remains the standard procedure for NMR signal processing. Nevertheless, new signal processing methods have been proposed during the same period of time including maximum entropy methods [1], linear prediction (LP) methods [2–4], and state space approaches [5–7]. Surveys of these methods may be found in [8–11]. Along with their better resolution capabilities, these so-called high resolution techniques present other advantages. In particular, most of them are non-iterative schemes, and they may yield directly the important parameters (frequencies, damping factors, amplitudes, and phases), without needing some deconvolution algorithm. Unfortunately, several drawbacks prevent them from replacing the FT. First, all of them generally require some trial-and-error adjustment, especially concerning the choice of the number of pertinent parameters (i.e., the order of the model). Second, the time spent for the computation is generally much longer than that of the FT. Finally, when the signals are of high complexity (i.e., made up of a great number of samples and/or containing a great number of resonances), all the problems become more crucial leading to a degradation of the overall performance. Moreover, in some situations, the problem may become actually untractable from a numerical point of view, because of the large amount of memory capacities requested.

* Corresponding author. Fax: +33-3-83-68-44-62.
E-mail addresses: el-hadi.djermoune@cran.uhp-nancy.fr (E.-H. Djermoune), marc.tomczak@cran.uhp-nancy.fr (M. Tomczak), pierre.mutzenhardt@rmn.uhp-nancy.fr (P. Mutzenhardt).

1090-7807/$ - see front matter © 2004 Elsevier Inc. All rights reserved.
doi:10.1016/j.jmr.2004.04.006

To overcome these problems, a natural approach consists in attempting to decompose the initial signal in several spectral subbands to replace a large eigenvalue problem by several small ones. Such a method, called LP-ZOOM, has been proposed in the NMR literature by Tang and Norris [12]. It is based upon LP applied on a single spectral window. More recently, a new approach named filter diagonalization method (FDM) has been introduced [13] which is comparable to the Matrix Pencil method [14]. It was then reformulated by Mandelshtam and Taylor [15] and further analyzed in several papers [16–18]. This method has the advantage to yield an estimate of the amplitudes without the need of a second least squares procedure. Another approach combining a uniform subband decomposition scheme and an ARMA estimation procedure was proposed in [19] and was shown to be efficient in processing long ^{13}C NMR signals. The latter two approaches share the same computational advantages than LP-ZOOM since both perform a local spectral analysis, but they are preferable from the point of view of estimation performances. Generally speaking, the idea of processing a signal by using small spectral windows has been known for a long time in the signal processing community. It is known as beamspacing in the array processing literature [20,21] and as subband decomposition or decimation in spectral analysis [22,23]. This technique may be seen as a preprocessing of the signal, and thus is independent from the method used for the estimation. In addition to their computational efficiency, subband techniques present several other advantages comparatively to a fullband estimation (i.e., achieved on the whole signal) [18,19,23–25].

Indeed, all these techniques are able to surpass the FT in estimation and detection performances when the corresponding parameters are properly chosen. Among these parameters, the degree of the decomposition will have strong influence on the detection rates, along with the order of the model considered (or equivalently the number of bases in the case of FDM). A solution to the problem of choosing the depth of the decomposition is given by adaptive approaches. The idea of an adaptive decomposition has been studied in a wide range of application domains including subband coding, noise suppression, spectral analysis, etc. Several papers have been published on the subject [24,26,27], using different kinds of criteria to achieve optimal decompositions. Most of them are based on the minimum description length (MDL) principle [24,28]: the decomposition is stopped if the estimated number of modes in a particular node is greater than the one obtained in its children. This technique is built to maximize (in theory) the number of detections. The problem which arises with such an approach is that it does not ensure that all the spectral information has been retrieved, because order criteria are not always reliable and what is worse, the decision is taken before the subband estimation. Thus, the resulting decomposition does not take into account the fact that an isolated mode may be estimated without needing a deeper decomposition. Now, this fact is particularly crucial for damped sinusoids since the damping factors increase with the degree of decimation and this could lead to an excessive spectral flatness.

The present work is intended to overcome this problem. It consists in a general strategy which can be applied with any estimation method, although it was originally developed as an improvement of the method proposed in [19]. The latter has been modified by adding a novel stopping rule to the decomposition process thus resulting in an adaptive approach. The criterion employed reflects the quality of the estimation in a given subband by evaluating the spectral flatness measure of the corresponding residuals. The decomposition is stopped only if the residuals are close to white noise, i.e., all local modes are retrieved. The resulting approach not only selects automatically the subbands where spectral peaks are present and reject the others, but also allows the algorithm to stop the decomposition on the bands where all modes may be easily extracted without the need of a deeper decomposition [29,30]. This is the main difference between the proposed adaptive approach and the existing ones. Obviously, the proposed strategy may also be extended to all subband-like techniques, including LP-ZOOM, FDM, and decimated signal diagonalization (DSD) [31], etc.

In Section 2 of this paper, some recalls about the uniform subband decomposition are presented: the main stages are set forth including the decomposition process itself and the estimation of subband parameters. Section 3 introduces the adaptive subband decomposition along with a new stop-criterion based on a measure of local spectral flatness of estimation residuals. In Section 4, some simulation trials are proposed to compare the performances of a fullband estimation and three different subband approaches. Then, in Section 5, the effectiveness of the method is demonstrated by analyzing raw carbon-13 experimental data (a synthetic mixture sample and a natural product sample). The results are compared to those obtained with FDM and a uniform decomposition using LPSVD or high-order Yule-Walker (HOYWSVD) as estimators. Finally, the conclusions are given in Section 6.

2. Uniform subband decomposition and parameter estimation

A free induction decay (FID) signal is a superposition of M damped complex exponentials in noise

$$y(n) = \sum_{k=1}^{M} h_k z_k^n + e(n), \tag{1}$$

for $n = 0, 1, \ldots, N-1$. Here $h_k = A_k \exp(j\phi_k)$ is the complex amplitude of mode $z_k = \exp(-\alpha_k + j\omega_k)$. The noise term $e(n)$ is often considered as zero-mean white noise sequence. The purpose of this work is to estimate the parameters M, z_k, and h_k from the noisy signal $y(n)$.

In this paper, the subband decomposition is considered as a pre-processing step obtained through filtering and decimation operations, although in the case of some methods such as FDM this processing is a part of the method itself. Different filterbanks may be considered, including wavelet packet structures [24] and overlapping schemes [20]. The main drawback of wavelet packets based filterbanks is that the problem of frequency aliasing is not taken into account. Now, it is well-known that if spectral aliasing occurs, it may lead to the attenuation or suppression of some modes [24] or resolution problems [30]. So we preferred to use the overlapping structure presented in [19,20] in which we admit 50% overlap between two successive filters. In [19], the decomposition was presented as a one-step operation using a decimation factor d. Recall that the decimation operation consists in retaining only one data sample from a set of d consecutive samples of a filtered signal. Now, if d is a power of 2, then exactly the same results may be obtained by performing successive decimations by 2 as will be explained below.

2.1. Multi-step decomposition

To simplify the decomposition procedure, the bands $[0, \pi]$ and $[-\pi, 0]$ of the original signal have to be processed separately. Concerning the band $[0, \pi]$, the decomposition is obtained as follows. Define:

$$y^{0,0}(n) \triangleq y(n) e^{-j\frac{\pi}{2}n}, \tag{2}$$

then the subband signals (or pseudo-FIDs) are given recursively by filtering and decimation operations, that is:

$$y^{i+1,2m}(n) = \sum_k g(k) y^{i,m}(2n-k) e^{j\frac{\pi}{4}(2n-k)}, \tag{3}$$

$$y^{i+1,2m+1}(n) = \sum_k g(k) y^{i,m}(2n-k) e^{-j\frac{\pi}{4}(2n-k)}, \tag{4}$$

where $g(n)$ is a lowpass filter with passband and stopband frequency edges verifying $\omega_p = \pi/4$ and $\omega_p < \omega_s \leqslant \pi/2$ (Fig. 1).

At the end of the decomposition, each subsignal $y^{i,m}(n)$, where $m = 0, 1, \ldots, 2^i - 1$, is associated to the frequency interval $[\frac{m\pi}{2^i}, \frac{(m+1)\pi}{2^i}]$ of the original signal. Of course, the same result could have been achieved by a one step decomposition with a decimation factor $d = 2^i$. Obviously, the number of data samples is decreased by a factor 2 at each iteration. Fig. 2 shows the decomposition tree and the correspondence between subband signals and the original signal. The (i, m) coordinates indicate the depth of the decomposition (i) and the frequency position of each band (m).

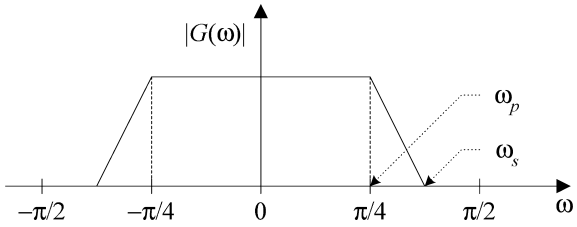

Fig. 1. Frequency response of the lowpass filter $g(n)$.

The decomposition of the band $[-\pi, 0]$ of the original signal can be obtained, in the same manner as before, by using $y^{0,0}(n) = y(n) e^{j(\pi/2)n}$. In this case, the resulting subsignals $y^{i,m}(n)$ correspond to the frequency interval $[-\frac{(m+1)\pi}{2^i}, -\frac{m\pi}{2^i}]$.

It can be easily shown that if a finite impulse response filter $g(n)$ is used, then the subband signal model is given by the following relation:

$$y^{i,m}(n) = \sum_{k=1}^{M'} h'_k z'^n_k + e^{i,m}(n), \tag{5}$$

for $n = 0, 1, \ldots, N'-1$, where N' is the number of subband samples. Here $M' \leqslant M$ is the number of resonances in the subband considered. The parameters h'_k and z'_k are the subband counterparts of the fullband parameters h_k and z_k for the band (i, m). The complex amplitude h'_k depends both on h_k and the filter shape. The subband mode z'_k is related to z_k by a frequency shift and an amplification of the damping factor $\left(|z'_k| = |z_k|^{2^i}\right)$. The way to obtain the fullband values from their subband equivalents will be given in the next section. The noise term $e^{i,m}(n)$ is a moving-average (MA) process of order $L - L/2^i$, where L is the order of the filter [19].

Note that the subband signals obtained from Eqs. (3) and (4) contain transient samples due to the (finite-time) filtering operation. This transient (with length $L/2$ for each filtering and decimation stage [19]) has to be suppressed to keep the model given in Eq. (5) valid. To do so, simply truncate the first $L/2$ samples from signals $y^{i,m}(n)$ before their next decomposition and *before* the estimation process.

2.2. Parameter estimation from subbands

The subband signal in Eq. (5) being a damped exponential signal in noise, the subband parameters z'_k and h'_k can be estimated using any high resolution method such as HOYWSVD [19], LPSVD [2], etc., although the use of the HOYWSVD is preferable due to the MA structure of the noise. Concerning the decimation filter, it can be shown to have a significant influence on the

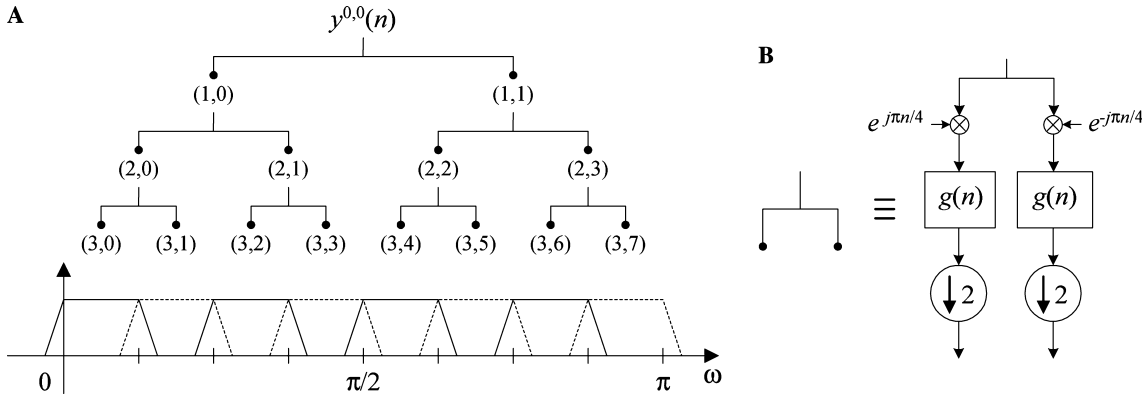

Fig. 2. (A) Uniform decomposition tree with successive decimations by a factor 2; (B) basic filter structure.

behavior of the singular values of the data (or autocorrelation) matrix. This leads common order estimators, such as the MDL criterion [32], to generally overestimate the number of components. To overcome this problem, just select the $p/2$ largest singular values and discard the $p/2$ smallest ones when evaluating such criteria [30], where p is the prediction order.

Once the subband parameters $\hat{z}'_k$ and $\hat{h}'_k$ in a given band (i,m) are estimated, they may be converted into their corresponding values in the fullband using the following equation [30]:

$$\begin{cases} \hat{z}_k = (\hat{z}'_k)^{1/2^i} \exp\left(\mathrm{j}\pi \frac{2m+1}{2^{i+1}}\right) & \text{for band } [0,\pi], \\ \hat{z}_k = (\hat{z}'_k)^{1/2^i} \exp\left(\mathrm{j}\pi\left(\frac{2m+1}{2^{i+1}} - 1\right)\right) & \text{for band } [-\pi,0]. \end{cases} \tag{6}$$

The fullband values of amplitudes may be similarly obtained from their subband images by a recursive relation

$$\hat{h}_k'^{i-1,[m/2]} = \frac{\hat{h}_k'^{i,m}}{(\hat{z}_k'^{i,m})^L G(\hat{z}_k'^{i,m})}, \tag{7}$$

where

$$\hat{z}_k'^{i,m} = \begin{cases} \hat{z}_k^{2^{i-1}} \exp\left(-\mathrm{j}\pi \frac{2[m/2]+1}{2}\right) \mathrm{e}^{\mathrm{j}\frac{\pi}{4}} & \text{for } m \text{ even}, \\ \hat{z}_k^{2^{i-1}} \exp\left(-\mathrm{j}\pi \frac{2[m/2]+1}{2}\right) \mathrm{e}^{-\mathrm{j}\frac{\pi}{4}} & \text{for } m \text{ odd} \end{cases} \tag{8}$$

and $[x]$ stands for the integer part of x. The fullband amplitude is then

$$\hat{h}_k = \hat{h}_k'^{0,0}. \tag{9}$$

2.3. Why an adaptive decomposition?

The subband decomposition approach was shown to have several advantages over a fullband estimation in the case of high complexity signals. The model orders considered are much smaller thus allowing one to handle with signals with large amounts of resonances and data. In addition, the frequency and dynamical resolutions are improved due to the separation of the spectral components in different bands, and what is more the detection rate is higher. The method operates at a lower SNR and presents a reduced variance as will be shown in Section 4. Finally, the numerical complexity is also decreased. Generally speaking, it was observed that the division of the initial problem into several sub-problems, each much more tractable, allows the estimation algorithms to give the full extent of their capabilities, thus surpassing the FT in detection performances [19]. Of course, all the performances strongly depend on the good choice of two parameters, namely the decimation factor and the prediction order.

In practice, it is first necessary to select manually the size and the position of the spectral windows in which the estimation must be performed or, in the case of a uniform decomposition, to choose the decimation factor d, thus the number of subbands and their sizes. This choice should be made in concordance with the signal encountered, which supposes some a priori knowledge, that is generally not available. Theoretically, the smaller is the size of the window the better are the overall performances (numerical complexity, resolution, estimation, and detection). But since the length of the pseudo-FIDs decreases with decreasing spectral window size, it is very likely that the estimation variance and detection performances will degrade themselves beyond a certain limit. Thus it is clear that there exist an optimal decimation factor. Since the subband decomposition is performed step-by-step, it is possible to decide at each level whether the decimation should be continued or not according to some criterion. The use of an adequate stop-criterion allows the decomposition to adapt itself to the spectral content of the subbands encountered resulting in an optimal (in the sense of the criterion) decomposition tree. The idea of an adaptive decomposition has been studied in several papers [24,26,27] and many stop-criteria have been considered, like order criteria, energy measures, entropy criteria, etc. Here we propose the use of a local spectral flatness based

stopping rule obtained by testing the whiteness of the subband residuals.

Concerning the prediction order, it is generally recommended to select it around $N'/2$ so as to achieve a minimum variance on the frequency estimate. In the case of a uniform decomposition, it is possible to do so provided that the length of the pseudo-FIDs N' is not too large. This is true for example when using a large decimation factor. Anyhow, in this paper we choose to first favor the maximization of the correct detection rate over the minimization of the frequency variance. This is achieved thanks to the adaptive decomposition using an adequate stop-criterion, thus making the choice of the prediction order less crucial. Once the decomposition tree is constructed, it is still possible to make a second estimation to optimize the variance. This will be further discussed in Section 3.3.

3. Adaptive subband decomposition

One of the advantages of an adaptive decomposition is that it enables one to stop the splitting of some bands in which the decimation does not bring profit in terms of detection of resonances or parameter accuracy. One can thus focus oneself on high complexity subbands in which the decomposition is relevant. So, the adaptive decomposition process is similar to the uniform one except that it may be stopped at any level for some bands according to a given stop-criterion. Fig. 3 shows the principle of such an approach.

3.1. The stop-criterion

Several stop-criteria have been already proposed, including order criteria [24,28], entropy and energy measures [26,33], etc. It was shown [29,30] that stop-criteria based on the properties of estimation residuals are preferable because they ensure better performances in terms of detection rate and estimation accuracy. The residuals in a given band (i,m) are defined as the difference between a subband signal and its estimate

$$\epsilon^{i,m}(n) = y^{i,m}(n) - \hat{y}^{i,m}(n) = y^{i,m}(n) - \sum_{k=1}^{\hat{M}'} \hat{h}'_k \hat{z}'^n_k, \tag{10}$$

for $n = 0, 1, \ldots, N'-1$. Here $\hat{M}'$ is the number of estimated modes in the subband considered. Ideally, if all modes have been retrieved (i.e., $\hat{M}' = M'$), then the residuals should be close to a white noise. If one or more modes are missed, then the sequence $\epsilon^{i,m}(n)$ is no more white. Several time-domain whiteness tests may be envisaged. Equivalently, it is possible to test the spectral flatness. The problem is that, in the case of the filterbank considered here, the residuals are not really white because of the filtering process. However, this non-white feature is particular: in the spectral domain, it can be seen that the spectral shape is only affected on the edges corresponding to the transition bands of the filter. So, in the frequency interval $[-\pi/2, \pi/2]$ corresponding to the filter's passband, the power spectral density (PSD) should still be considered as flat if the residuals do not contain modes any more. Thus, by considering a local spectral flatness test, i.e. restricted to the passband of the filter, it is possible to make a decision about stopping or continuing the decomposition process.

3.2. The measure of flatness

A lot of spectral flatness tests have been proposed among which Fisher's whiteness test [34] is the most popular. In the case of damped complex exponentials signals, we found that Drouiche's test [35] is more appropriate because of a better detection rate [30]. The latter is based on the periodogram estimate of the PSD of $\epsilon^{i,m}(n)$ defined by

$$\hat{P}_{N'}(\omega) = \frac{1}{2\pi N'} \left| \sum_{n=0}^{N'-1} \epsilon^{i,m}(n) \mathrm{e}^{\mathrm{j}n\omega} \right|^2. \tag{11}$$

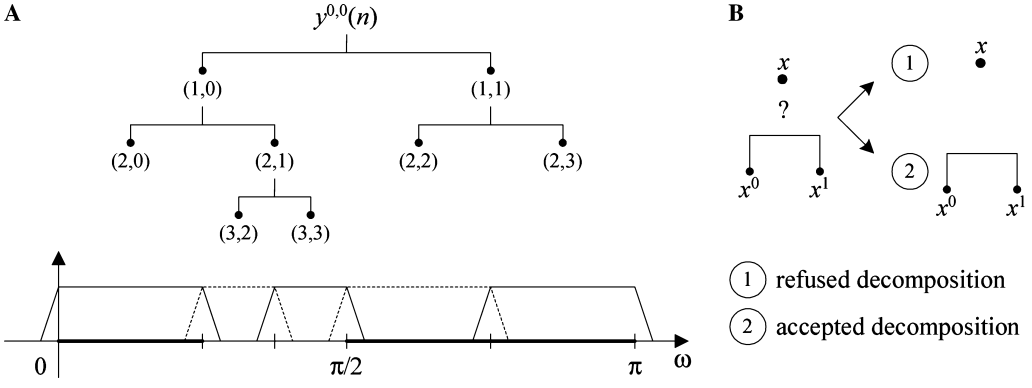

Fig. 3. (A) Adaptive decomposition tree and corresponding non-uniform subbands; (B) stopping rule principle.

The measure of spectral flatness, restricted to the interval $[-\pi/2, \pi/2]$, is given by the following quantity [35]:

$$\hat{W}_{N'} = \ln\frac{1}{\pi}\int_{-\frac{\pi}{2}}^{\frac{\pi}{2}} \hat{P}_{N'}(\omega)\,\mathrm{d}\omega - \frac{1}{\pi}\int_{-\frac{\pi}{2}}^{\frac{\pi}{2}} \ln \hat{P}_{N'}(\omega)\,\mathrm{d}\omega - \gamma, \quad (12)$$

where γ is the Euler constant ($\gamma = 0.57721$). To decide whether or not $\hat{P}_{N'}(\omega)$ is flat (or constant), the quantity $\hat{W}_{N'}$ is compared to a threshold t_α which is fixed according to the desired false alarm rate α by using the following relation:

$$t_\alpha = \sqrt{\frac{2(\pi^2/6 - 1)}{N'}}\,\mathrm{erf}^{-1}(1 - 2\alpha), \quad (13)$$

where $\mathrm{erf}^{-1}(x)$ is the inverse of the standard error function. The false alarm rate α is a free parameter. In this paper, it is fixed to 1%. The decision about stopping or carrying on the decomposition is then taken according to the following rule:

$$\begin{cases} \hat{W}_{N'} < t_\alpha & \rightarrow \quad \text{stop}, \\ \hat{W}_{N'} \geqslant t_\alpha & \rightarrow \quad \text{continue}. \end{cases} \quad (14)$$

3.3. Implementation issues

When using the proposed method, it is first necessary to choose a prediction order p for the estimation algorithm. In the case of uniform decomposition or fullband estimation, the latter must be chosen carefully because it is directly related to the number of components and samples. In the case of a *single undamped mode* and at high SNR, it has been shown that the optimal choice of p (in the sense of the minimization of the frequency variance), for nearly all the estimation methods, is $p = N'/3$ or $p = 2N'/3$ where N' is the number of sub- or fullband data samples [14,36,37]. This result was then generalized for multiple undamped sinusoids and it is now admitted that the optimal p is around $N'/2$, provided that the modes are well separated and the SNR is high. Now, in the case of a *damped sinusoid*, the minimum variance is reached only when $p = N'/3$ for the LP method [38].

When the adaptive approach is considered, there are two ways to choose this parameter [25]. We can for example choose $p = N/3$ in the fullband (N is the number of total data samples) and then divide it by 2 as the decomposition gets deeper. This tuning is used for example in [16,17] where the spectral windows are implicitly assumed to be sufficiently small but it is not attractive in our case because of the large matrices involved in the first steps of the decomposition. Another approach consists in using the same prediction order for all decimation levels (i.e., all subband signals) [25]. In this case, the role of the stopping rule is to obtain the set of subbands (spectral windows) in which the prediction order chosen will be *convenient*, because the method is able to adapt itself to the local content of the signal. Indeed, if the order is too small, the decomposition will be deeper because the algorithm will tend to the situation where the average number of peaks in each subband corresponds roughly to the order selected. On the contrary, if the order is too large, it will become sufficient at an early stage and the decomposition process will be shorter. As a rule of thumb, for experimental signals, the prediction order has been chosen as a fraction (say 1/3 or 1/2) of the expected total number of lines M, provided that $N \gg M$.

Of course, this discussion concerns the maximization of the detection rate and not the minimization of the estimation variance. But since the stopping rule performs also an a posteriori validation by measuring the distance of the residuals to a white noise, the decomposition does not stop until the estimated parameters are close to the true ones. So the algorithm does not ensure a minimum variance but it is clear that the variance cannot be far from its minimum. Anyhow, since the detection rate is maximized, it is still possible to rerun the algorithm (only in the subbands retained by the method at first run) by choosing the theoretical optimal p to minimize also the variance. Note that, for all the experimental signals we have analyzed, this step had not led to significant improvements in the estimation results.

The only other choice that the user has to make is concerning the false alarm rate for the stop criterion. The latter is generally fixed in the literature between 1 and 10%. From our experience, this parameter is far from being critical when chosen in the previous interval since it influences little the final decimation level and not at all the estimation performances. In our simulations, we always use $\alpha = 1\%$.

The method proposed is now briefly summarized.

(1) Choose the band to be decomposed ($[0, \pi]$ or $[-\pi, 0]$).
(2) Perform one step of the subband decomposition using Eqs. (3) and (4).
(3) For each resulting band do the following
   (a) obtain the subband parameters h'_k and z'_k from, for example, LPSVD or HOYWSVD,
   (b) generate the residuals (Eq. (10)),
   (c) compute t_α and evaluate the flatness (Eqs. (13) and (14)),
   (d) if residuals are white then this band is a terminal one and the decomposition should be stopped, otherwise the decomposition must be continued.
(4) Search for a decomposable band from the whole tree.
(5) Repeat step 2, until no decomposable band is found.
(6) Convert all the subband parameters into their fullband values.

Note that a Matlab implementation of this algorithm is available from the authors on request. The

present method will now be applied to a simulation example and then to two experimental ^{13}C NMR signals.

4. Simulation example

The aim of this section is to give an illustration of the advantages of subband decomposition over a fullband estimation and of the superiority of adaptive decompositions over uniform ones. The simulation signal used here consists in 2 damped exponentials in zero-mean white noise. The two components, which frequencies are set to 0.11 and 0.15, as in [24], have both the same amplitude and a damping factor of 0.015. The peak SNR is varying between 0 and 20 dB. For each SNR value, multiple simulations have been performed using 100 realizations of the additive noise. The results achieved using the suggested adaptive subband decomposition are compared to those obtained with three other approaches. The first considers the MDL-based adaptive decomposition proposed in [24], the second uses a uniform decomposition and the third performs a fullband estimation. Each approach uses the HOYWSVD estimation method. Results achieved when using the LPSVD method can be found in [29]. All approaches are compared on the basis of their estimation variances, their miss ratios and their percentage of terminal bands relatively to the uniform decomposition. The miss ratio is defined as the percentage of modes not detected.

The prediction order is initially fixed to 64 and is then divided by 2 between two successive levels. This particular choice of the order is intended here to make the fullband estimation not too penalized. Results achieved are presented on Fig. 4. In terms of variance, it appears that at low SNR, the subband estimations are better than the fullband one, the adaptive approaches yield a lower frequency variance than the uniform one, and the proposed adaptive approach leads to the lowest variance. At high SNR, the global approach performs better than all other approaches, which could be expected in view of the rather large prediction order used with regard to the number of components. But, it can be seen that the proposed approach tends to show the same behavior as the fullband one.

From the point of view of detection, it can be observed that subband approaches are always superior to the fullband one. The proposed approach yields the smallest miss ratio. This is because the decomposition is stopped when the total decimation factor is "optimal" in the sense that further decimation does not improve the detection rate and may even make the estimation performances decrease.

Finally, concerning the computational load, Fig. 4C shows that the MDL-based one leads to the decomposition of 5 bands, while our approach leads to decompose only two of the eight bands.

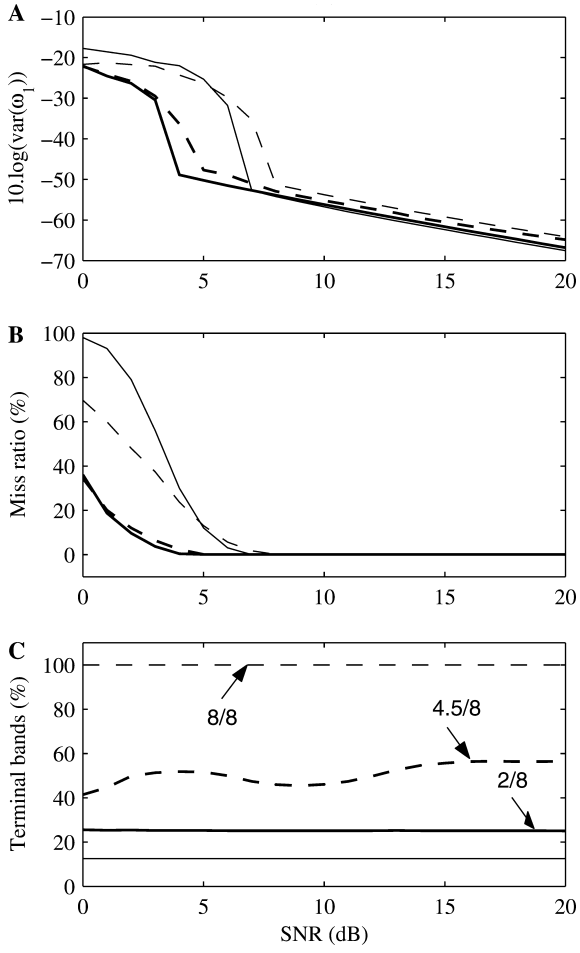

Fig. 4. Results achieved on simulation signal. (A) Variance of frequency ω_1; (B) miss ratio; and (C) percentage of terminal bands. (—), Fullband estimation; (– –), uniform subband decomposition; (–), proposed adaptive approach; and (– –), MDL–based adaptive decomposition.

5. Experimental results

In this section, results achieved on experimental ^{13}C NMR signals are presented. At first, the uniform and adaptive decompositions are compared, along with FDM, on a signal called NMR1, resulting from quantitative experiments on a synthesized mixture of 19 compounds in $CDCl_3$, with TMS as the internal reference (see [19] for details about the sample). This signal is complex enough to reveal important differences between the uniform and the adaptive subband approaches.

Second, we consider a set of signals named NMR2, corresponding to a natural substance (gypsogenin 3-*O*-glucuronide extracted from the root of *Silene vulgaris*) in pyridine-D6 (see [39] for details). These signals are obtained using different numbers of accumulations. This

allows us to point out the superiority of our approach over the FT at low SNR.

5.1. Signal NMR1

Regarding the present analysis, the main features of signal NMR1 are its length (128 k) and the number of peaks (104). For this signal, a fullband estimation via high resolution methods is nearly impossible because of the large amount of data and of the relatively high number of resonances [19]. Thus, we only consider uniform and adaptive subband approaches. For uniform decompositions, the signal is split into 256 spectral windows between 0 and 0.5. This is obtained, in the case of FDM, via 256 contiguous rectangular windows of equal size. In each spectral window $[f_{\min}, f_{\max}]$, the Fourier basis size is fixed according to $K_{\text{win}} = N(f_{\max} - f_{\min})/2$. For HOYWSVD and LPSVD, the prediction order is set to $p = 60$ in each subband. In the case of the adaptive approach, only HOYWSVD and LPSVD are considered, both using a prediction order $p = 60$. The results are shown in Table 1. It can be seen that, for a uniform grid, the HOYWSVD method is always better than LPSVD and FDM in terms of correct detections but at the expense of a larger false detection rate. Obviously, the adaptive approach enables one to improve both the good detection and the false alarm rates. Finally, it appears clearly that the computational burden is drastically reduced with the adaptive approach. Indeed, the total number of bands analyzed is diminished from 256 to 45 or 57 depending on the estimator considered.

Table 1
Results achieved on signal NMR1

Decomposition	Estimation	Detected modes		Bands	
		Good	False	Stopped	Total
Uniform	HOYWSVD	94	23	0	256
	FDM	90	5	0	256
	LPSVD	90	6	0	256
Adaptive	HOYWSVD	95	7	43	45
	LPSVD	93	3	54	57

The proposed adaptive decomposition detects more components and generates less subbands than the uniform one.

The decomposition tree obtained with the adaptive decomposition approach and the HOYWSVD estimator is shown on Fig. 5. One can easily observe that the decomposition tracks the spectral bands where information is localized and that the "empty" bands are stopped at low decimation levels. The resulting residuals are almost white, which indicates that nearly all resonances were (well) extracted. For example, it can be seen that, in the bands [0.21875, 0.25] and [0.3125, 0.34375], the decomposition is stopped early because no modes are present. Indeed, the decomposition gets deeper in the spectral intervals containing several close modes (e.g., in the region around 0.15). Finally, in some cases, there is

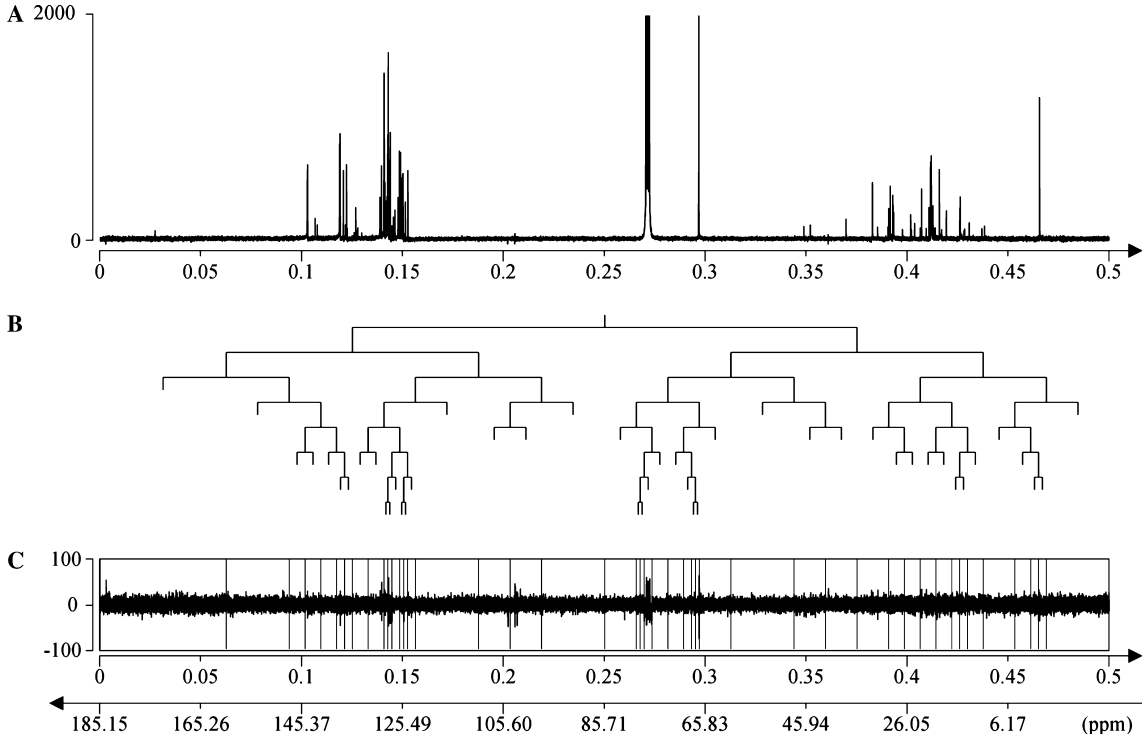

Fig. 5. Adaptive decomposition of signal NMR1. (A) Absorption spectrum; (B) decomposition tree; and (C) estimation residuals per band. The decomposition tree tracks the bands where peaks are present.

only one line but the decomposition gets even so deeper (e.g., line between 0.45 and 0.5). This is because either the frequency or the amplitude of this line was not accurately estimated at earlier stages.

Results achieved using the adaptive approach associated to the HOYWSVD estimator, and FDM, are partially shown in Table 2 together with the theoretical lines and those obtained in [19]. In terms of accuracy on the frequency estimates, it is clear that all approaches are comparable. The estimation error is of the order of 10^{-5}. Line 56 was not detected by the uniform subband methods (including FDM) but was detected by the adaptive one. Note that, lines 72, 73a, 74a, 74, 76, and 76a corresponds to false detections (they do not appear in the theoretical line list). Finally, from the point of view of amplitudes, the three approaches yield roughly the same estimates except for one or two cases (lines 39 and 55). One can observe that, near the lines associated to the solvent (lines 73, 75, and 77), the spurious peaks detected by the uniform approaches have rather large

Table 2
Results achieved in some frequency intervals of signal NMR1

Line	Theoretical		Uniform		FDM		Adaptive	
	δ (ppm)	I (%)	f	A (%)	f	A (%)	f	A (%)
...	...	...	...	...	...	...	...	...
6	144.26	32.05	0.10277	34.87	0.10277	37.79	0.10277	33.33
7	144.23	24.45	0.10286	44.31	0.10286	50.14	0.10285	39.46
8	144.22	17.10	—	—	—	—	—	—
9	144.06	42.38	0.10303	40.92	0.10303	41.79	0.10303	36.45
...	...	...	...	...	...	...	...	...
31	129.11	43.37	0.14073	41.88	0.14073	39.90	0.14072	40.40
32	129.06	100.00	0.14092	100.00	0.14092	100.00	0.14092	100.00
33	128.94	39.40	0.14124	44.53	0.14124	39.43	0.14124	35.96
34	128.72	24.45	0.14181	25.99	0.14181	22.91	0.14181	22.36
35	128.47	22.98	0.14239	20.57	0.14238	35.58	0.14239	21.92
36	128.37	50.86	0.14266	52.06	0.14266	53.03	0.14266	48.16
37	128.31	64.11	0.14275	61.54	0.14275	67.93	0.14275	59.37
38	128.25	100.00	0.14293	94.19	0.14293	71.99	0.14293	94.41
39	128.23	22.98	0.14296	34.53	0.14297	104.01	0.14297	31.77
40	128.23	24.45	0.14301	29.07	0.14300	38.36	0.14301	44.52
41	128.15	25.19	0.14315	25.92	0.14315	30.80	0.14315	25.76
42	128.07	1.70	—	—	—	—	—	—
43	127.88	5.08	0.14381	7.46	0.14382	6.09	0.14382	4.81
44	127.86	64.11	0.14392	64.41	0.14392	70.79	0.14392	58.77
...	...	...	...	...	...	...	...	...
50	126.06	50.38	0.14848	47.19	0.14848	69.18	0.14848	43.71
51	126.03	7.42	0.14851	27.34	—	—	0.14851	13.19
52	125.95	42.38	0.14861	44.22	0.14861	46.19	0.14861	39.36
53	125.81	5.08	0.14903	2.01	0.14901	8.81	0.14902	7.16
54	125.80	48.70	0.14906	55.16	0.14907	52.95	0.14906	46.31
55	125.72	34.20	0.14931	33.47	0.14931	35.26	0.14931	30.14
56	125.63	11.49	—	—	—	—	0.14955	1.86
57	125.62	0.85	—	—	—	—	—	—
58	125.59	32.05	0.14958	50.67	0.14958	52.26	0.14959	41.79
59	125.45	7.42	0.14996	8.30	0.14997	9.36	0.14996	7.28
60	125.38	43.37	0.15006	38.66	0.15006	41.92	0.15006	37.04
61	125.33	50.00	0.15028	49.36	0.15028	50.44	0.15028	49.35
62	125.23	3.52	0.15052	3.62	—	—	0.15052	3.58
63	124.85	24.45	0.15146	25.78	0.15146	20.10	0.15146	20.91
...	...	...	...	...	...	...	...	...
72			0.27026	1.02	0.27037	164.75		
73	77.30		0.27063	2012.26	0.27063	1948.82	0.27063	1898.45
73a					0.27068	2460.37		
74a					0.27074	301.65		
74			0.27086	10.77			0.27086	69.25
75	77.00		0.27143	2003.53	0.27143	2165.82	0.27143	1899.61
76			0.27151	11.99				
76a					0.27203	395.39		
77	76.70		0.27223	2038.43	0.27223	2169.71	0.27223	1854.96
...	...	...	...	...	...	...	...	...

Comparison with the results obtained in [19] and those achieved by FDM.

amplitudes. This is because the estimation methods tend to fit broad resonances by several narrower ones.

The total calculation time of the adaptive approach was of 1 min with the HOYWSVD estimator and of 30 s with LPSVD (on a PC Pentium at 2.4 GHz), that is a little shorter than with the uniform approaches.

5.2. Signal NMR2

The set of signals NMR2, with length 64 k, is obtained using a number of accumulations (N_a) which varies between 1 and 2048. For example, the spectra corresponding to $N_a = 16$, 512, and 2048 are shown in Fig. 6. The experimental data are always corrupted by some spurious peaks due to instrumentation and which can occur whatever the number of accumulations is. These lines being very narrow, their corresponding modes are close to undamped sinusoids, so they are not retained by the HOYWSVD method, which makes use of the unit circle criterion [19]. They can be easily recognized in Fig. 6 as they do not follow the accumulation process. For the sake of clarity, they have been starred in the figure.

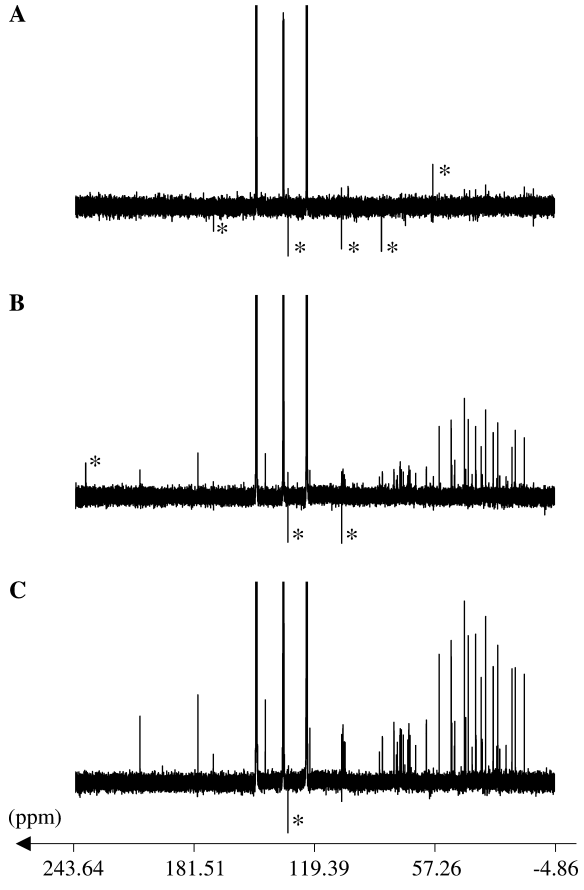

Fig. 6. Absorption spectra of signals NMR2. (A) $N_a = 16$; (B) $N_a = 512$; and (C) $N_a = 2048$. For illustrative purpose, the signals presented in this figure are phase corrected and their baselines are suppressed, but the signals used for the trials were not corrected before being processed. (*) indicate spurious peaks.

For this example, the number of accumulations necessary to retrieve all of the 45 spectral lines using the FT is 2048. Table 3 shows the results obtained for $N_a = 256$, 512, 1024, and 2048 (lines corresponding to the solvent are not presented). One can observe that our adaptive approach combined with HOYWSVD detects

Table 3
Results achieved on signals NMR2 as a function of the number of accumulations

Line	Theoretical	Estimated frequencies			
	δ (ppm)	256	512	1024	2048
1	10.85	0.03163	0.03163	0.03163	0.03163
2	15.52	0.04098	0.04099	0.04099	0.04099
3	17.25	0.04447	0.04447	0.04448	0.04447
4	20.29	0.05058	0.05060	0.05061	0.05059
5	23.55	0.05721	0.05715	0.05715	0.05715
6	24.58	0.05921	0.05920	0.05920	0.05920
7	25.02	0.06015	0.06012	0.06015	0.06013
8	27.01	0.06412	0.06412	0.06412	0.06412
9	30.87	0.07191	0.07191	0.07191	0.07191
10	32.64	0.07554	0.07558	0.07556	0.07558
11	33.17	0.07655	0.07655	0.07655	0.07655
12	35.86	0.08191	0.08189	0.08192	0.08192
13	36.06	0.08231	0.08231	0.08232	0.08231
14	37.90	0.08594	0.08596	0.08599	0.08599
15	39.94	0.09011	0.09012	0.09011	0.09011
16	41.25	0.09279	0.09276	0.09276	0.09276
17	41.94	0.09415	0.09415	0.09415	0.09415
18	46.83	0.10398	0.10399	0.10399	0.10399
19	47.09	0.10452	0.10455	0.10453	0.10453
20	48.36	0.10712	0.10709	0.10709	0.10709
21	48.70	0.10773	0.10773	0.10773	0.10773
22	54.96	0.12037	0.12037	0.12037	0.12037
23	61.64	0.13377	0.13374	0.13375	0.13375
24	67.08	0.14483	0.14481	0.14479	0.14479
25	70.05	0.15071	0.15070	0.15069	0.15070
26	70.66	0.15194	0.15197	0.15197	0.15197
27	71.21	0.15296	0.15301	0.15298	0.15299
28	73.51	0.15774	0.15775	0.15773	0.15774
29	74.48	0.15963	0.15963	0.15964	0.15964
30	75.09	0.16091	0.16090	0.16090	0.16090
31	75.28	0.16130	0.16130	0.16130	0.16130
32	76.59	—	0.16394	0.16395	0.16395
33	77.02	—	0.16487	0.16488	0.16488
34	78.29	0.16733	0.16741	0.16741	0.16740
35	78.37	—	0.16754	0.16750	0.16752
36	84.30	0.17946	0.17945	0.17946	0.17945
37	85.94	0.18266	0.18264	0.18266	0.18266
38	103.61	0.21831	0.21835	0.21836	0.21836
39	104.03	0.21917	0.21920	0.21919	0.21920
40	104.76	0.22063	0.22064	0.22064	0.22064
41	121.90	0.25504	0.25505	0.25506	0.25506
42	145.00	0.30159	0.30159	0.30159	0.30159
43	171.90	0.35576	0.35574	0.35572	0.35571
44	179.90	0.37181	0.37180	0.37180	0.37181
45	209.84	0.43209	0.43210	0.43212	0.43213
Correct detections		42	45	45	45

The proposed approach detects all of the modes from $N_a = 512$ whereas the FT becomes exploitable at $N_a = 2048$.

all resonances for $N_a \geqslant 512$. So, the adaptive subband decomposition ensures detection performances equivalent to those achieved with a Fourier approach, but at a much lower SNR. In addition, the accuracy of the estimated frequencies do not vary much between $N_a = 512$ and $N_a = 2048$ as may be seen on Table 3. The maximal deviation between frequencies estimated at $N_a = 512$ and $N_a = 2048$ is 3×10^{-5} (lines 12, 14, 43, and 45). Thus, the necessary number of accumulations may be approximately divided by a factor 4, which corresponds for this experiment to an acquisition time of 15 min instead of 1 h. So, generally, the subband decomposition approach allows one to expect an important reduction of experimentation times.

6. Conclusion

This paper presents an almost automated, fast, and non-iterative procedure to estimate directly the parameters of NMR from time-data. It is based upon a subband decomposition of the initial signal and the use of standard identification methods such as LPSVD and HOYWSVD techniques. The decomposition is realized in an adaptive fashion thanks to a new stop-criterion consisting in a local flatness test of the subband estimation residuals.

It is known that subband decomposition has several advantages in terms of detection rate, frequency resolution, and numerical complexity relatively to fullband estimators. Moreover, this technique is able to handle with signals of high complexity (i.e., long FIDs with many resonances). The adaptive scheme proposed in the present paper, further improves the performances of the subband decomposition in the sense that there is no more need to select the decimation factor. Indeed, the method automatically selects the signal-bearing bands and decides whether or not a band should be further decomposed. Furthermore, the method is more robust to changes on the prediction order and the estimation variance is "controlled" by the a posteriori validation involved by the stop-criterion. Finally, this approach is more efficient in terms of calculation time because of the rejection of empty bands.

The results achieved on a simulation example were compared to those obtained with two other decomposition schemes and a fullband method. It appeared that the performances of the proposed algorithm are actually better from the point of detection as well as estimation variance. Two experimental signals were also considered. On the first one, the method was compared with the corresponding uniform approach and FDM. It was observed that the adaptive approach improves the detection rate and decreases both the false detection rate and the numerical complexity. On the second signal, it was shown that the method performs better than the FT at low SNR, which allows one to expect a notable decrease of experimentation time.

Finally, it must be pointed out that the computation times did not exceed 1 min, even on long signals with a hundred resonances. One could think that this is a long time as compared to the fast FT, but one should remind that the FT does not give a direct access to the relevant parameters. Moreover, the latter requires some other pre- and post-processing like phase and baseline corrections and peak-picking.

Acknowledgments

The authors thank the reviewers for their remarks and critics that helped us to improve the presentation of this work.

References

[1] E.D. Laue, J. Skilling, J. Staunton, Maximum entropy reconstruction of spectra containing antiphase peaks, J. Magn. Reson. 63 (1985) 418–424.
[2] H. Barkhuijsen, R. de Beer, W.M.M.J. Bovée, D. van Ormondt, Retrieval of frequencies, amplitudes, damping factors, and phases from time-domain signals using a linear least-squares procedure, J. Magn. Reson. 63 (1985) 465–481.
[3] H. Gesmar, J.J. Led, Spectral estimation of complex time-domain NMR signals by linear prediction, J. Magn. Reson. 76 (1988) 183–192.
[4] J. Tang, J.R. Norris, Linear prediction z-transform (LPZ) method, Padé rational approximation, and the Burg maximum entropy extrapolation, J. Magn. Reson. 78 (1988) 23–30.
[5] H. Barkhuijsen, R. de Beer, D. van Ormondt, Improved algorithm for noniterative time domain model fitting to exponentially damped magnetic resonance signals, J. Magn. Reson. 73 (1987) 553–557.
[6] W. Pijnappel, A. van den Boogaart, R. de Beer, D. van Ormondt, SVD-based quantification of magnetic resonance signals, J. Magn. Reson. 97 (1992) 122–134.
[7] S. van Huffel, H. Chen, C. Decaniere, P. van Hecke, Algorithm for time-domain NMR data fitting based on total least squares, J. Magn. Reson. Ser. A 110 (1994) 228–237.
[8] D.S. Stephenson, Linear prediction and maximum entropy methods in NMR spectroscopy, Prog. NMR Spectr. 20 (1988) 515–626.
[9] D.N. Rutledge, Signal Treatment and Signal Analysis in NMR, Elsevier Science, New York, 1996.
[10] J.C. Hoch, A.S. Stern, NMR Data Processing, Wiley-Liss, New York, 1996.
[11] P. Koehl, Linear prediction spectral analysis of NMR data, Prog. NMR Spectr. 34 (1999) 257–299.
[12] J. Tang, J.R. Norris, LP-ZOOM, a linear prediction method for local spectral analysis of NMR signals, J. Magn. Reson. 79 (1988) 190–196.
[13] M.R. Wall, D. Neuhauser, Extraction, through filter-diagonalization, of general quantum eigenvalues or classical normal mode frequencies from a small number of residues or a short-time segment of a signal. I. Theory and application to a quantum-dynamics model, J. Chem. Phys. 102 (20) (1995) 8011–8022.
[14] Y. Hua, T.K. Sarkar, Matrix pencil method for estimating parameters of exponentially damped/undamped sinusoids in

noise, IEEE Trans. Acoust. Speech Signal Process. 38 (5) (1990) 814–824.
[15] V.A. Mandelshtam, H.S. Taylor, Harmonic inversion of time signals and its applications, J. Chem. Phys. 107 (17) (1997) 6756–6769.
[16] V.A. Mandelshtam, H.S. Taylor, A.J. Shaka, Application of the filter diagonalization method to one- and two-dimensional NMR spectra, J. Magn. Reson. 133 (1998) 304–312.
[17] H. Hu, Q.N. Van, V.A. Mandelshtam, A.J. Shaka, Reference deconvolution, phase correction, and line listing of NMR spectra by the 1D filter diagonalization method, J. Magn. Reson. 134 (1998) 76–87.
[18] V.A. Mandelshtam, FDM: the filter diagonalization method for data processing in NMR experiments, Prog. NMR Spectr. 38 (2001) 159–196.
[19] M. Tomczak, E.-H. Djermoune, A subband ARMA modeling approach to high-resolution NMR spectroscopy, J. Magn. Reson. 158 (2002) 86–98.
[20] S.D. Silverstein, W.E. Engeler, J.A. Tardif, Parallel architectures for multirate superresolution spectrum analyzers, IEEE Trans. Circ. Syst. 38 (4) (1991) 449–453.
[21] M.D. Zoltowski, G.M. Kautz, S.D. Silverstein, Beamspace Root-MUSIC, IEEE Trans. Signal. Process. 41 (1) (1993) 344–364.
[22] M.P. Quirk, B. Liu, Improving resolution for autoregressive spectral estimation by decimation, IEEE Trans. Acoust. Speech Signal Process. 31 (1983) 630–637.
[23] W.M. Steedly, C.-H.J. Ying, R.L. Moses, A modified TLS-Prony method using data decimation, IEEE Trans. Signal Process. 42 (1994) 2292–2303.
[24] C. van den Branden Lambrecht, M. Karrakchou, Wavelet packet-based high-resolution spectral estimation, Signal Process. 47 (1995) 135–144.
[25] S. Rao, W. Pearlman, Analysis of linear prediction, coding, and spectral estimation from subbands, IEEE Trans. Inform. Theory 42 (1996) 1160–1178.
[26] R.R. Coifman, M.V. Wickerhauser, Entropy-based algorithms for best basis selection, IEEE Trans. Inform. Theory 38 (2) (1992) 713–718.
[27] D.L. Donoho, I.M. Johnstone, Ideal spatial adaptation via wavelet shrinkage, Biometrika 81 (1994) 425–455.
[28] L.T. Mainardi, D. Origgi, P. Lucia, G. Scotti, S. Cerutti, A wavelet packets decomposition algorithm for quantification of in vivo ^{1}H-MRS parameters, Med. Eng. Phys. 24 (2002) 201–208.
[29] E.-H. Djermoune, M. Tomczak, An adaptive subband decomposition method for high resolution nuclear magnetic resonance spectroscopy, in: Proceedings of the third International Symposium on Physics in Signal Image Processing, Grenoble, France, 2003, pp. 193–196.
[30] E.-H. Djermoune, Estimation des paramètres de sinusoïdes amorties par décomposition en sous-bandes adaptative. Application à la spectroscopie RMN, Ph.d. thesis, Université Henri Poincaré, Nancy 1, France, 2003.
[31] D. Belkic, P.A. Dando, H.S. Taylor, J. Main, Decimated signal diagonalization for obtaining the complete eigenspectra of large matrices, Chem. Phys. Lett. 315 (1-2) (1999) 135–139.
[32] M. Wax, T. Kailath, Detection of signals by information theoretic criteria, IEEE Trans. Acoust. Speech Signal Process. 33 (1985) 387–392.
[33] R. Coifman, Y. Meyer, S. Quake, M.V. Wickerhauser, Signal processing and compression with wave packets, Technical report, Numerical Algorithms Research Group, Yale University, 1990.
[34] M.B. Priestley, Spectral Analysis and Time Series, sixth ed., Academic Press, London, 1989.
[35] K. Drouiche, A new test for whiteness, IEEE Trans. Signal Process. 48 (7) (2000) 1864–1871.
[36] A.C. Kot, S. Parthasarathy, D.W. Tufts, R.J. Vaccaro, The statistical analysis of state-variable balancing and Prony's method in parameter estimation, in: IEEE International Conference on Acoustics Speech Signal Processing, 1987, pp. 1549–1552.
[37] B.D. Rao, K.S. Arun, Model based processing of signals: A state space approach, Proc. IEEE 80 (2) (1992) 281–309.
[38] A. Okhovat, J.R. Cruz, Statistical analysis of the Tufts-Kumaresan and principal Hankel components methods for estimating damping factors of single complex exponentials, in: IEEE International Conference on Acoustics Speech Signal Processing, 1989, pp. 2286–2289.
[39] S. Bouguet-Bonnet, M. Rochd, P. Mutzenhardt, M. Henry, Total assignment of 1H and 13C NMR spectra of three triterpene saponins from roots of Silene vulgaris (Moench) Garcke, Magn. Reson. Chem. 40 (2002) 618–621.